

Single Particle Strengths and Mirror States in ^{15}N – ^{15}O below 12.0 MeV

C.E. Merten¹, D.D. Caussyn¹, A.M. Crisp¹, N. Keeley²,
K.W. Kemper¹, O. Momtyuk¹, B.T. Roeder¹, and A. Volya¹

¹*Department of Physics, Florida State University, Tallahassee, FL, 32312*

²*National Centre for Nuclear Research, Andrzej Soltana 7, 05-400 Otwock, Poland*

New $^{14}\text{N}(\text{d},\text{p})$ angular distribution data were taken at a deuteron bombarding energy of 16 MeV to locate all narrow single particle neutron states up to 15 MeV in excitation. A new shell model calculation is able to reproduce all levels in ^{15}N up to 11.5 MeV and is used to characterize a narrow single particle level at 11.236 MeV and to provide a map of the single particle strengths. The known levels in ^{15}N are then used to determine their mirrors in the lesser known nucleus ^{15}O . The $2s_{1/2}$ and $1d_{5/2}$ single particle centroid energies are determined for the ^{15}N – ^{15}O mirror pair as: ^{15}N ($2s_{1/2}$) = 8.08 MeV, ^{15}O ($2s_{1/2}$) = 7.43 MeV, ^{15}N ($1d_{5/2}$) = 7.97 MeV, and ^{15}O ($1d_{5/2}$) = 7.47 MeV. These results confirm the degeneracy of these orbits and that the ^{15}N – ^{15}O nuclei are where the transition between the $2s_{1/2}$ lying below the $1d_{5/2}$ to lying above it, takes place. The $1d_{3/2}$ single particle strength is estimated to be centered around 13 MeV in these nuclei.

PACS numbers: 21.60.Cs, 21.10.Jx, 25.45.Hi

I. INTRODUCTION

It was realized early in the development of theoretical nuclear structure models [1] that the ^{15}N nucleus is an ideal candidate for study because considerable experimental work had shown that there existed seven positive parity states that might be described as a closed 1p shell with a single 2s or 1d shell particle outside its core. In addition, the large energy gap between the ground and first excited state, 5.3 MeV, similar to the 6 MeV gap in ^{16}O , reinforced the idea of ^{15}N having a closed core for its ground state. It was also pointed out in Halbert and French [1], one of the first shell model calculations describing the low lying positive parity states, that many levels in ^{15}N could be populated by a large variety of inelastic and particle transfer reactions making this nucleus ideal for testing details of future model calculations. Later, weak coupling model calculations [2, 3] focused on the positive parity states with the goal of extending the understanding of these states up to 10 MeV in excitation. While the first works included only 1p-2h configurations it was argued by Shukla and Brown [4] that contributions from 3p-4h states were needed to describe several of the levels below 10 MeV and the work of Lie *et al.* [3] confirmed this idea. Lie *et al.* [3] also proposed that spin parity assignments could be made by comparing theoretical calculations with the measured properties of levels and in further work Lie and Engeland [5] extended calculations for both positive and negative parity levels up to 13 MeV in excitation. An excellent test for these extended calculations was their comparison with the three particle transfer reactions $^{12}\text{C}(^7\text{Li},\alpha)$ [6] and $^{12}\text{C}(^6\text{Li},^3\text{He})$ [7] where both reactions selectively populate states including an especially strongly populated one at 10.69 MeV with much more strength than would be consistent with the known $3/2^-$ level. The large angular momentum mismatch of the ($^6\text{Li},^3\text{He}$) reaction favored the population of a high spin state, which was then matched to a $9/2^+$

state calculated by Lie and Engeland [5] close to this excitation energy and having a large 3p-4h component. Concurrently, a $^{14}\text{C}(\text{p},\gamma)$ study discovered a new resonance at 10.693 MeV in excitation and gave it a $9/2^+$ assignment, and its decay reported in Ref. [8] was subsequently used to demonstrate that three particle transfer reactions [9] do indeed strongly populate this 3p-4h, $9/2^+$ state as predicted by theory.

This work reports new data for the $^{14}\text{N}(\text{d},\text{p})$ reaction taken at a bombarding energy of 16 MeV to locate all narrow neutron single particle states up to 15 MeV in excitation. It continues the ideas of the early shell model theoretical studies with the goal of testing a modern calculation against the known level structure of ^{15}N and then to use this calculation along with the new $^{14}\text{N}(\text{d},\text{p})$ data to identify all single particle levels up to 12 MeV in excitation. These firm spin parity assignments are then used to determine their mirror levels in the lesser known nucleus ^{15}O [10]. The analysis of the present single neutron data and that from a recently published $^{14}\text{N}(^3\text{He},\text{d})$ proton transfer study [11] are combined to determine the $2s_{1/2}$ and $1d_{5/2}$ centroid energies in the ^{15}N – ^{15}O mirror pair. With these results, a reasonable estimate is made for the concentration of the $1d_{3/2}$ strength in these nuclei. The single particle centroid energies of the mass 15 nuclei are particularly interesting because they are in the cross over region where the $2s_{1/2}$ orbit lies below the $1d_{5/2}$ orbit in ^{13}C , and above it in ^{17}O . An analysis of an early extensive $^{14}\text{N}(\text{d},\text{p})$ study [12] showed these orbits to be almost degenerate in ^{15}N . However, the published spectrum showed possible single particle states for which no analysis of spectroscopic strength was carried out, suggesting the possibility that some strength for these orbits might lie at a higher excitation energy than studied to date. The present higher energy (d,p) work was designed to search for this possible missing strength. The extraction of these centroid energies adds to our knowledge of the evolution of the s-d shell orbits as a function of pro-

ton and neutron number, the importance of which has been detailed in a recent publication of Hoffman *et al.* [13].

II. EXPERIMENTAL PROCEDURE

Cross sections for the $^{14}\text{N}(\text{d,p})^{15}\text{N}$ reaction were obtained by bombarding a melamine ($\text{C}_3\text{H}_6\text{N}_6$) target of about $300 \mu\text{g}/\text{cm}^2$ on a $20 \mu\text{g}/\text{cm}^2$ carbon backing with a 16 MeV deuteron beam produced by the FSU tandem-linac accelerator combination. Data were also collected on a carbon target at the same angles as for the melamine to separate its contribution to the higher excitation ^{15}N spectra from the melamine, the main experimental thrust of the current work. A $\Delta\text{E-E}$ silicon detector telescope was used to measure the outgoing protons and deuterons and a single silicon detector on the opposite side of the incoming beam served as a monitor of the target conditions. The deuteron beam current was limited to 15 nA to make certain that there was no loss of target due to beam heating during the data collection. Elastic scattering and transfer data were also taken at deuteron beam energies of 9, 10, and 12 MeV to extract absolute cross sections and to check these cross sections with previously published (d,p) data [12]. To make use of previously published ^{12}C and ^{14}N deuteron elastic scattering data to establish the absolute cross section for the (d,p) reaction, it was necessary to adopt a procedure to separate the two peak yields since the elastic peak contained yield from both nuclei, most notably at forward angles. To extract the carbon yield from the total peak, the ratio of the yield for the 4.4 MeV first excited state in ^{12}C to that for the ^{12}C ground state for the deuteron scattering by the carbon target was found at all measured angles. The elastic nitrogen yield was determined by extracting the 4.4 MeV yield from the melamine target and then using the yield ratio from the carbon target to subtract its contribution to the total nitrogen plus carbon elastic yield. For the angles 25° , 30° and 35° it was possible to separate the yields from carbon and nitrogen which provided a direct check on the ratio technique. The relative elastic scattering angular distributions for both carbon and nitrogen were normalized to optical model calculations based on previously published elastic scattering data [14] for both nuclei to extract a normalization constant that establishes the absolute cross section for the (d,p) transfer reactions. The error in the absolute cross sections in Ref. [14] is 15% which is taken as the absolute error here.

A typical $^{14}\text{N}(\text{d,p})$ spectrum showing the population of ^{15}N states up to 15 MeV in excitation is displayed in Figure 1. Also shown are the energies for the various particle decay thresholds for ^{15}N . Note also in the spectrum the contribution from the $^{12}\text{C}(\text{d,p})$ peaks and the strong peak arising from the hydrogen in the target. Figure 1 also shows the $^{12}\text{C}(\text{d,p})$ spectrum below that from the melamine demonstrating that the narrow peaks above 10 MeV are indeed from the $^{14}\text{N}(\text{d,p})$ reaction. All

the narrow peaks below 11.5 MeV in excitation reported earlier in Phillips and Jacobs [12] were observed in the present work including the narrow peaks at 10.066 and 11.236 MeV, whereas those at 12.145 and 12.493 MeV were not. The 11.236 MeV angular distribution was not included in the analysis of Ref. [12]. It was not possible to extract an angular distribution for the small peak in the spectrum at 10.80 MeV in excitation because of its weak population and its being obscured at many angles by the nearby peak from the hydrogen in the target. In contrast with various multiparticle transfer reactions that selectively populate narrow peaks up to 20 MeV in excitation in ^{15}N , no strong isolated peaks are observed in the $^{14}\text{N}(\text{d,p})$ spectrum above 12.5 MeV in excitation. While there appears to be a broad peak around 14.5 MeV in excitation, it was not possible to prove conclusively that it was not from the known broad $3/2^+$ state at 8.2 MeV in ^{13}C [15]. Data were taken in the laboratory angular range from 10° to 35° in 5° steps to produce angular distributions for extracting the orbital angular momentum transfer and the single particle spectroscopic factors that provide a measure of the neutron single particle strength for a given state. The size of the relative errors in the angular distribution data are either smaller or equal to the size of the data points or are shown.

III. SHELL MODEL CALCULATIONS

The present work reports the results of new ^{15}N shell model calculations that used an unrestricted 1p-2s1d shell valence space with an interaction Hamiltonian taken from the work of Utsuno and Chiba [16]. Time dependent and traditional shell model procedures were used with the computer code COSMO [17] to perform the calculations. The known and calculated states in ^{15}N are given in the first two columns of Table I, where it can be seen that all known levels can be paired with calculated ones. The number in parenthesis besides that for a given spin and parity refers to the theoretical level ordering so that for example $5/2^+$ (3) is the third $5/2^+$ level and its known partner is found at 9.155 MeV. Figure 2 displays the difference between the known and calculated levels. The energies of the calculated positive parity states are fairly well predicted by the calculations, but the energies of the negative parity states are higher than their corresponding experimental ones.

IV. DWBA CALCULATIONS

Zero-range distorted-wave Born approximation (ZR-DWBA) calculations were performed using the code DWUCK4 [18]. The DWUCK4 code enables the use of the technique of Vincent and Fortune [19] for handling the target-like overlap when the final state in the residual nucleus is unbound and the incorporation of a non-locality correction factor β for the distorted waves and

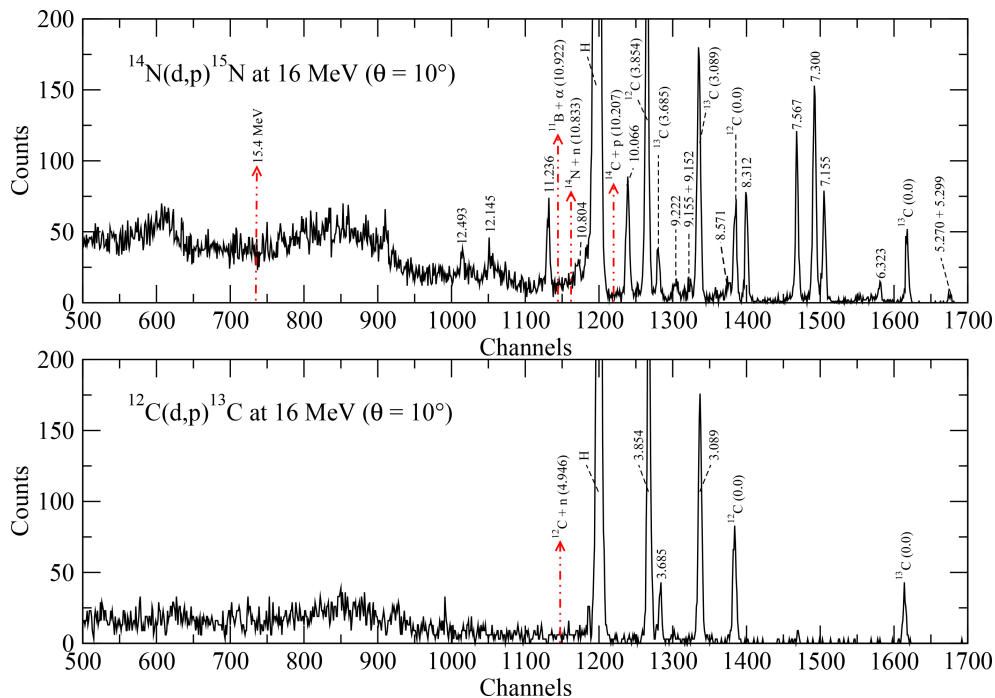


FIG. 1. (color online) Typical spectra from the present work, shows the $^{14}\text{N}(d,p)^{15}\text{N}$ and $^{12}\text{C}(d,p)^{13}\text{C}$ spectra at 10° taken with a beam energy of 16 MeV. The $^{12}\text{C}(d,p)$ spectra was gainshifted to match the peak height of the 3.854 MeV state in ^{13}C to show matching peaks. Separation energies have also been added to each spectra.

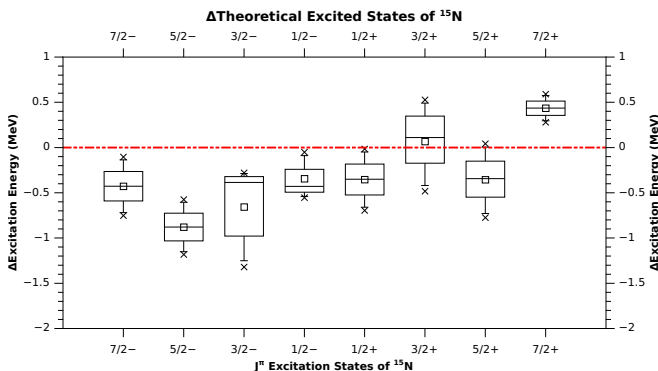


FIG. 2. (color online) Distribution of the theoretical calculations in relation to the experimentally observed excitation energies in ^{15}N . The dashed line at zero denotes a match in energy values.

transferred particle bound state. Deuteron and proton optical model potentials were taken from the study of Phillips and Jacobs [12]. The $\langle^{15}\text{N}|^{14}\text{N} + n\rangle$ overlaps were calculated using binding potentials of Woods-Saxon form and parameters $r_0 = 1.25$ fm, $a_0 = 0.65$ fm and a Thomas spin-orbit term with strength $\lambda = 25$. A value of $D_0^2 = 1.55 \times 10^4$ MeV² fm³ and a finite-range correction factor of 0.621 fm were used, as recommended in the DWUCK4 manual for (d,p) reactions. Non-locality corrections [20] with $\beta = 0.54$ fm for the deuteron and $\beta = 0.85$ fm for the proton and transferred neutron were also applied.

For unbound states, calculations assuming the transferred neutron to be in an $\ell = 0$ state employed the weak binding energy approximation (WBEA), i.e. the $\langle^{15}\text{N}|^{14}\text{N} + n\rangle$ overlap was calculated assuming a binding energy of 0.1 MeV, although the correct excitation energy of the state was used for the “kinematic” part of the calculation. A similar procedure also had to be adopted for the 12.145 MeV and 12.493 MeV unbound states when the transferred neutron was assumed to be in an $\ell = 1$ state since it was not possible to find resonances for these states under this assumption, the single-particle widths being too wide. However, the Vincent-Fortune technique [19] was employed to calculate the $\ell = 2$ angular distributions for these two states and both the $\ell = 1$ and $\ell = 2$ angular distributions for all the other unbound states. For those calculations where the WBEA had to be used no non-locality corrections were employed since their influence on the result is likely to be smaller than the effect of using $\langle^{15}\text{N}|^{14}\text{N} + n\rangle$ overlaps calculated under the somewhat crude assumptions of the WBEA. Normalization factors were extracted for each transition by multiplying each calculated transfer cross section by a number until the two magnitudes matched. This normalization factor is then the single particle spectroscopic factor C^2S . Transitions to $3/2^+$ states can proceed by either $\ell = 0$ or $\ell = 2$ transfers and in these cases the normalizations for the two transfers were varied until the value of χ^2 that combined the two calculations was minimized.

TABLE I. Assigned Mirror States in ^{15}N and ^{15}O with Energy Differences

^{15}N		Theoretical $^{15}\text{N}^\dagger$		^{15}O		ΔE (MeV)	ΔE (MeV)
E (MeV)	J^π	E (MeV)	J^π (n)	E (MeV)	J^π	^{15}N	$^{15}\text{N}-^{15}\text{O}$
5.270	$5/2^+$	5.227	$5/2^+$ (1)	5.241	$5/2^+$	0.043	0.029
5.299	$1/2^+$	5.994	$1/2^+$ (1)	5.183	$1/2^+$	-0.695	0.166
6.324	$3/2^-$	6.602	$3/2^-$ (1)	6.176	$3/2^-$	-0.279	0.148
7.155	$5/2^+$	7.370	$5/2^+$ (2)	6.859	$5/2^+$	-0.215	0.296
7.300	$3/2^+$	6.772	$3/2^+$ (1)	6.793	$3/2^+$	0.528	0.508
7.567	$7/2^+$	6.976	$7/2^+$ (1)	7.276	$7/2^+$	0.591	0.291
8.312	$1/2^+$	8.327	$1/2^+$ (2)	7.557	$1/2^+$	-0.015	0.756
8.571	$3/2^+$	8.638	$3/2^+$ (2)	8.284	$3/2^+$	-0.067	0.287
9.050	$1/2^+$	9.400	$1/2^+$ (3)	8.743	$1/2^+$	-0.350	0.307
9.152	$3/2^-$	9.474	$3/2^-$ (2)	8.922	$3/2^-$	-0.322	0.230
9.155	$5/2^+$	9.929	$5/2^+$ (3)	8.922	$5/2^+$	-0.774	0.233
9.222	$1/2^-$	9.273	$1/2^-$ (2)	8.982	$1/2^-$	-0.051	0.242
9.760	$5/2^-$	10.335	$5/2^-$ (1)	9.488	$5/2^-$	-0.575	0.272
9.829	$7/2^-$	10.580	$7/2^-$ (1)	9.660	$7/2^-$	-0.751	0.169
9.925	$3/2^-$	10.310	$3/2^-$ (3)	9.609	$3/2^-$	-0.385	0.316
10.066	$3/2^+$	9.779	$3/2^+$ (3)	9.484	$3/2^+$	0.287	0.582
10.450	$5/2^-$	11.631	$5/2^-$ (2)	10.290	$5/2^-$	-1.181	0.160
10.533	$5/2^+$	11.005	$5/2^+$ (4)	10.300	$5/2^+$	-0.472	0.233
10.693	$9/2^+$	12.292	$9/2^+$ (1)	10.461	$9/2^+$	-1.600	0.229
10.702	$3/2^-$	12.022	$3/2^-$ (4)	10.480	$3/2^-$	-1.320	0.222
10.804	$3/2^+$	11.286	$3/2^+$ (4)	10.506	$3/2^+$	-0.482	0.298
11.236	$7/2^+$	10.956	$7/2^+$ (2)	10.917	$7/2^+$	0.280	0.318
11.293	$1/2^-$	11.846	$1/2^-$ (3)	11.025	$1/2^-$	-0.553	0.267
Avg Diff						-0.365	0.285

\dagger (n) denotes the order which the J^π state appeared in the calculations.

V. RESULTS

TABLE II. Spectroscopic Factors for the $^{14}\text{N}(\text{d,p})^{15}\text{N}$ Reaction

E (MeV)	$\ell(\hbar)$	J^π	Orbit	C^2S		
				16 MeV	Theoretical	9 MeV ^a
0.00 (g.s.)	1	$1/2^-$	p _{1/2}	1.31	1.14	—
5.280	0	$1/2^+$	s _{1/2}	0.03(02)	0.39	< 0.05
	2	$5/2^+$	d _{5/2}	0.14(01)	0.11	< 0.05
6.323	1	$3/2^-$	p _{3/2}	0.22(01)	—	0.10(02)
	2	$5/2^+$	d _{5/2}	1.06(02)	0.65	0.88(03)
7.300	0	$3/2^+$	s _{1/2}	0.98(03)	0.72	0.89(04)
	2		d _{5/2}	0.19(03)	—	0.07(05)
7.567	2	$7/2^+$	d _{5/2}	0.96(02)	0.73	0.87(01)
8.312	0	$1/2^+$	s _{1/2}	1.10(05)	0.64	1.02(04)
	2		d _{3/2}	0.10(04)	—	< 0.09
8.571	0	$3/2^+$	s _{1/2}	0.07(02)	—	0.02(01)
	2		d _{5/2}	0.13(02)	0.20	0.12(03)
10.066	0	$3/2^+$	s _{1/2}	0.32(04)	—	0.32(08)
	2		d _{5/2}	0.65(02)	0.55	0.48(08)
11.236	2	$7/2^+$	d _{5/2}	0.20(01)	—	—
12.493	2	$5/2^+$	d _{3/2}	0.28(01)	—	—
	2		d _{5/2}	0.30(01)	—	—

^a Data extracted from [12].

The current experimental set up was optimized to look for structure in the experimental spectrum above 10 MeV in excitation so that no data were taken for the ground state transition. For completeness in the current analysis, data taken by Schiffer *et al.* [21] in a survey of ground state (d,p) transitions in 1p shell nuclei at a deuteron bombarding energy of 12 MeV were also analyzed. As can be seen in Figs. 3–5, the angular distributions are well described by the DWBA calculations. The descriptions of both the 7.300 ($3/2^+$) and 8.312 ($1/2^+$) angular distributions are improved by slight addition of an $\ell = 2$ transfer to the dominant $\ell = 0$ transfer. An $\ell = 2$ contribution to the 8.312 MeV transition can only occur from a $1d_{3/2}$ neutron configuration which would yield a component of this orbit much lower than expected but its addition at less than 10% of the dominant $\ell = 0$ component is determined primarily by the small cross section to this state at the angular distribution minimum which results in a large error associated with the extraction of this component.

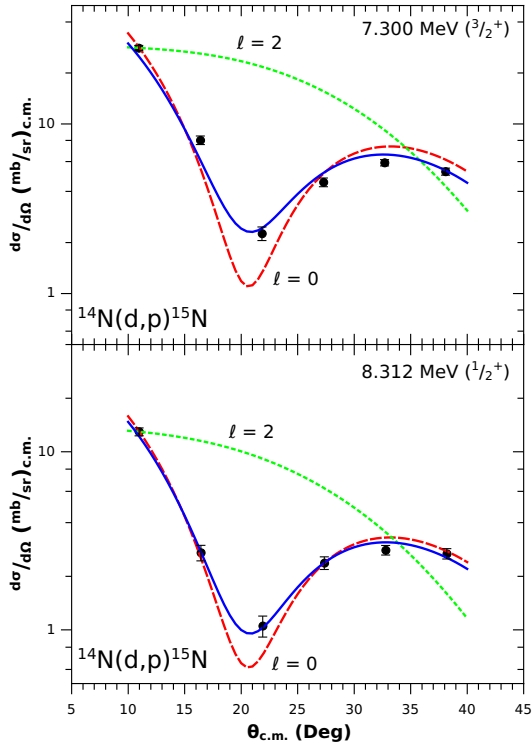


FIG. 3. (color online) Angular distribution for states in ^{15}N which were determined to be $\ell = 0$ dominant.

TABLE III. Currently reported states in ^{15}N and $^{15}\text{O}^a$

^{15}N		^{15}O	
E (MeV)	J^π	E (MeV)	J^π
5.270	$5/2^+$	5.241	$5/2^+$
5.299	$1/2^+$	5.183	$1/2^+$
6.324	$3/2^-$	6.176	$3/2^-$
7.155	$5/2^+$	6.859	$5/2^+$
7.300	$3/2^+$	6.793	$3/2^+$
7.567	$7/2^+$	7.276	$7/2^+$
8.312	$1/2^+$	7.557	$1/2^+$
8.571	$3/2^+$	8.284	$3/2^+$
9.050	$1/2^+$	8.743	$1/2^+$
9.152	$3/2^-$	—	—
9.155	$5/2^+$	8.922	$5/2^+$
—	—	8.922	$1/2^+$
9.222	$1/2^-$	8.982	$(1/2^-)$
—	—	9.484	$(3/2^+)$
9.760	$5/2^-$	9.488	$5/2^-$
9.829	$7/2^-$	9.660	$(7/2^-, 9/2^-)$
9.925	$3/2^-$	9.609	$3/2^-$
10.066	$3/2^+$	—	—
10.450	$5/2^-$	10.290	$(5/2^-)$
10.533	$5/2^+$	10.300	$5/2^+$
10.693	$9/2^+$	10.461	$(9/2^+)$
10.702	$3/2^-$	10.480	$(3/2^-)$
10.804	$3/2^+$	(10.506)	$(3/2^+)$
11.236	$\geq 3/2$	10.917	$7/2^+$

^a Data extracted from [10].

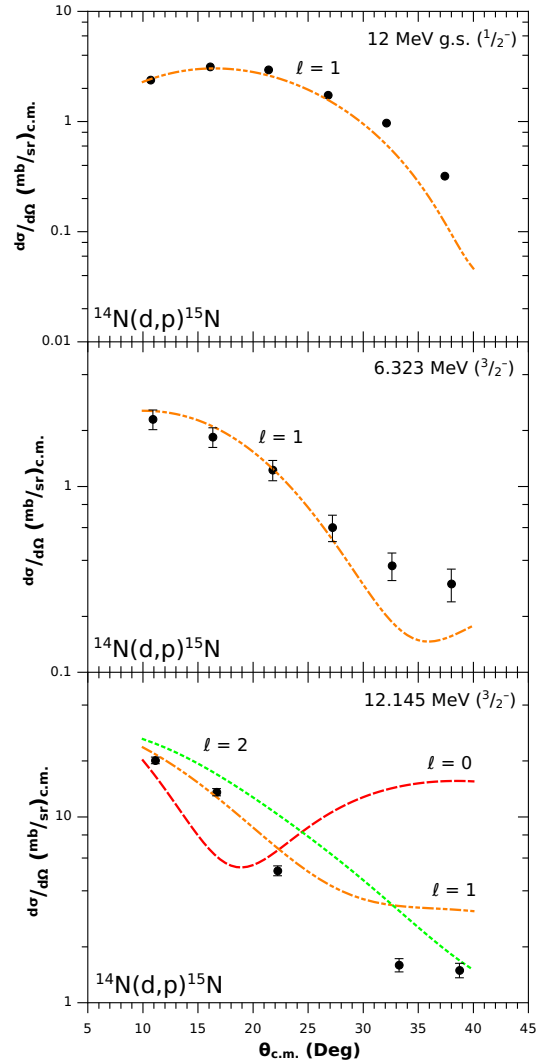


FIG. 4. (color online) Angular distribution for states in ^{15}N which were determined to be $\ell = 1$ dominant.

The only calculated level below 11.5 MeV for which there is no known experimental equivalent is the $7/2^+$ (2) predicted to lie at 10.956 MeV. The angular distribution for the 11.236 peak is well described by an $\ell = 2$ transfer which is consistent with a spin of $7/2^+$. This assignment would also agree with the most recent compilation for mass 15 [10] which has the 11.236 MeV state listed as having a spin greater than or equal to $3/2$. Further support for this assignment can be found by considering the width of a possible single particle level in a Woods-Saxon potential well. If the spin of the 11.236 MeV level were either $1/2^+$ or $3/2^+$, both allowed for an $\ell = 2$ transfer, then they would have an $\ell = 0$ component which would require a width for this state of 300 keV or so, whereas the measured width is 3.3 keV. If it were $5/2^+$, then it would be the fifth $5/2^+$ level and one sees that the $5/2^+$ single particle strength is exhausted by this excitation energy, leaving $7/2^+$ (2) as the remaining choice. The

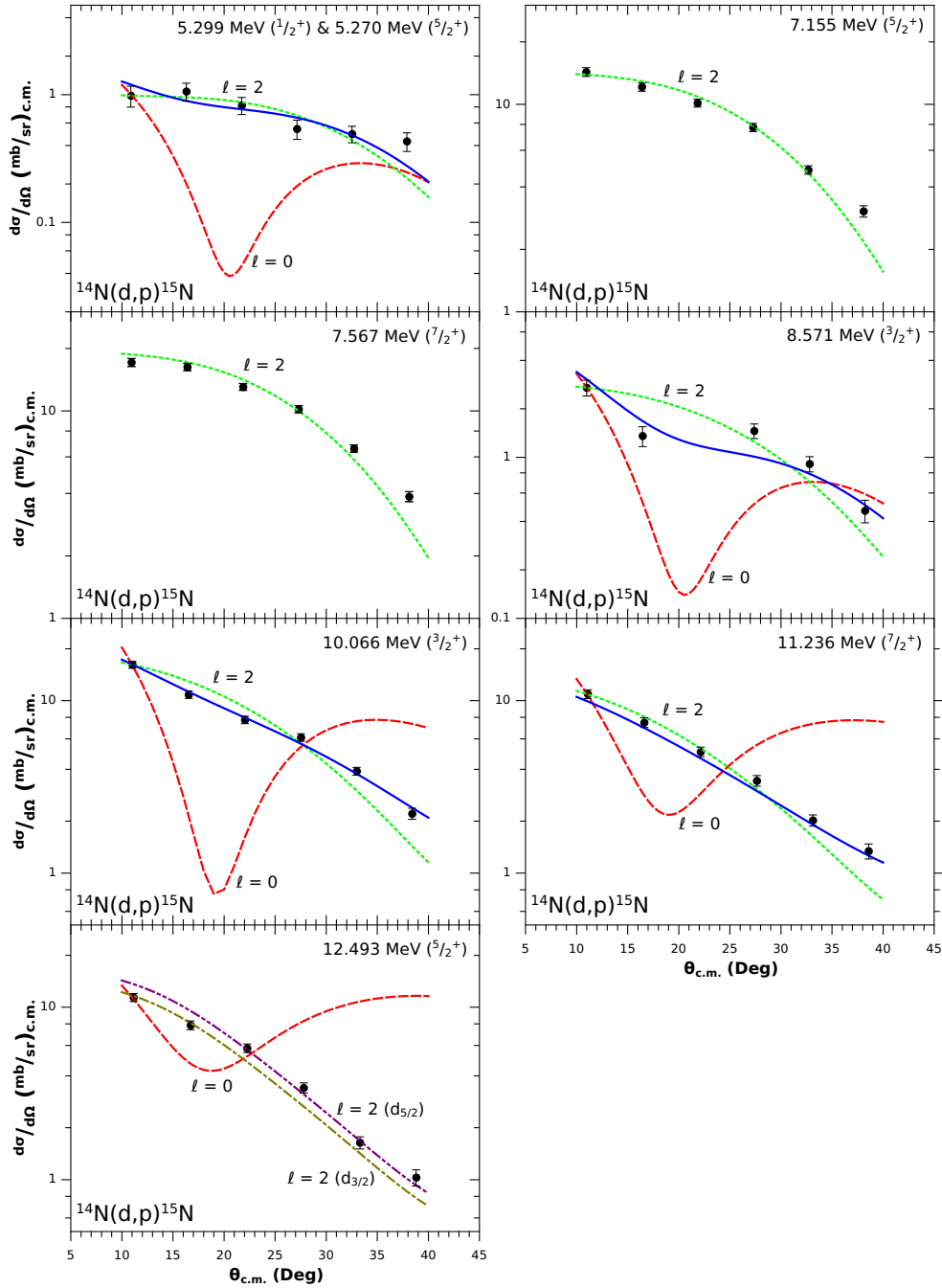


FIG. 5. (color online) Angular distribution for states in ^{15}N which were determined to be $\ell = 2$ dominant.

shell model calculation has a spectroscopic factor of 0.71 for $7/2^+$ (1) and 0.135 for $7/2^+$ (2) and 0.009 for $7/2^+$ (3) again supporting the $d_{5/2}$ $7/2^+$ component for this level.

The compilation [10] shows a $5/2^+$ state at 12.493 MeV which is consistent with the present $\ell = 2$ angular distribution analysis. However, whether it is a remnant of the $1d_{5/2}$ orbit or the beginning of the single particle strength for the $1d_{3/2}$ orbit cannot be determined from the present work. Comparison with the $^{12}\text{C}(d,p)$ analysis of Ohnuma *et al.* [15] suggests that it is the beginning of the $1d_{3/2}$

orbit. The present spectroscopic factors with the corresponding errors arising from the fit to the data along with those obtained by Phillips and Jacobs are given in Table II. A reanalysis of both the ground state and excited states from the previously published data in Refs. [12, 21] resulted in agreement between the two analyses giving considerable confidence in their values.

The experimentally determined excitation energy concentrations of neutron single particle strengths for the $2s_{1/2}$ and $1d_{5/2}$ orbits is well reproduced by the shell model

calculations as displayed in Figure 6. The energy scale begins at 5 MeV of excitation in ^{15}N . This figure shows that both the $2s_{1/2}$ and $1d_{5/2}$ strengths lie within the first 5-10 MeV of excitation and are concentrated in just a few strong levels, consistent with the experimental data. In fact the dominant single particle strength is quickly exhausted as the nuclear excitation increases so that a positive parity state such as the third $5/2^+$ state at 9.155 MeV is almost unobservable in the (d,p) spectrum. In contrast, the $1d_{3/2}$ single particle strength is spread out over a region of about 4 MeV and is about 5 MeV above the centroid of the lower two orbits. In addition levels with the majority of the $1d_{3/2}$ single particle strength are expected to be quite wide since they will be 3–5 MeV above the $^{14}\text{N} + n$ separation energy of 10.8 MeV and difficult to identify.

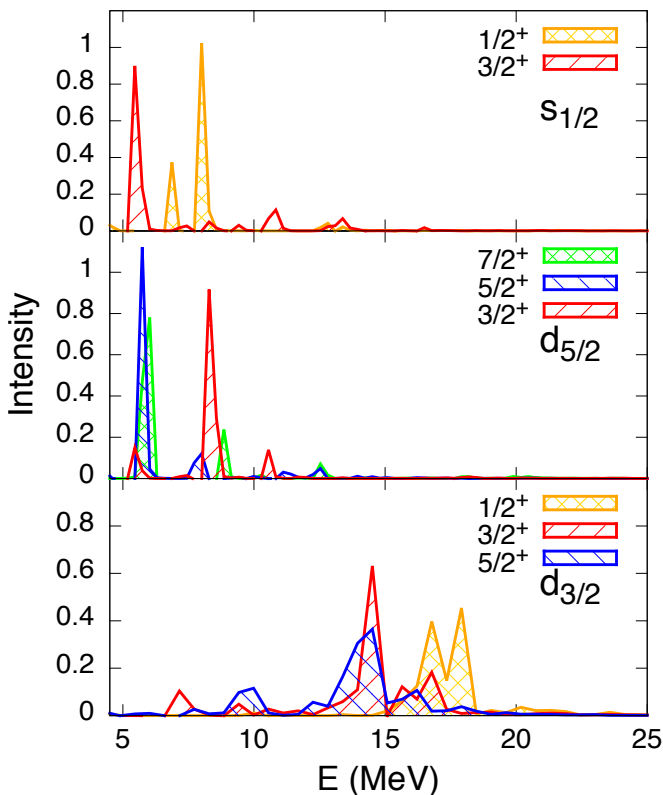


FIG. 6. (color online) Plot from the theoretical calculations showing where the dominant $2s_{1/2}$, $1d_{5/2}$, and $1d_{3/2}$ states are located in relation to the excitation energy in ^{15}N .

VI. MIRROR LEVELS IN $^{15}\text{N}-^{15}\text{O}$

The structure of the $^{15}\text{N}-^{15}\text{O}$ nuclei has been studied both experimentally and theoretically for many years now. However, there are still levels at relatively low excitation energy (\sim less than 12.5 MeV) in ^{15}O whose spin and parities are not determined. There are also levels that exist in one or the other of these mirror nuclei but

with no corresponding partner in the other. Table III lists levels in ^{15}N and ^{15}O up to 11 MeV in excitation from the current compilation [10] with possible pairings based on their known properties and energy differences. The levels in ^{15}O are on average 0.283 MeV below those for ^{15}N as determined from the known low lying levels in both nuclei. The uncertainties in the listed levels for the mirrors $^{15}\text{N}-^{15}\text{O}$ become readily apparent above about 9 MeV in Table III.

The 9.152 MeV level in ^{15}N with a well established $3/2^-$ assignment has no known mirror in ^{15}O . There are two levels at 8.922 MeV in ^{15}O with one being the $5/2^+$ mirror level of the ^{15}N 9.155 MeV level and the other assigned as $1/2^+$ in ^{15}O but with no corresponding ^{15}N mirror. Early reviews [5, 22] showed this level in ^{15}O as $1/2^-$. The reason for the change of assignment to $1/2^+$ is not readily apparent from a review of the literature from the time of this change. The present mirror level would assign $3/2^-$ to the second 8.922 MeV level with its mirror being the 9.152 MeV $3/2^-$ level in ^{15}N . The ^{15}O level listed at 9.484 ($3/2^+$) has no known mirror in ^{15}N and is probably the same as the 9.488 $5/2^-$ level with its ^{15}N mirror being at 9.76 MeV. While the current compilation has the spin-parity assignments for the ^{15}O levels at 8.98, 9.829, 10.066, 10.29, 10.461, 10.48 and 10.506 in brackets, (see Table III), mirror levels in ^{15}N all have firm assignments which then allows these brackets to be removed. In addition, the 9.66 MeV level in ^{15}O is assigned as $7/2^-$ based on its mirror 9.829 in ^{15}N . The present $^{14}\text{N}(d,p)$ study along with the shell model calculations presented earlier assign $7/2^+$ to the 11.236 MeV ^{15}N level. Its mirror at 10.917 in ^{15}O has a firm assignment of $7/2^+$ supporting this assignment. Table I gives the final level assignments in the mirrors $^{15}\text{N}-^{15}\text{O}$ from the present work.

VII. $2s_{1/2}$ AND $1d_{5/2}$ SINGLE PARTICLE CENTROID ENERGIES IN $^{15}\text{N}-^{15}\text{O}$

From the present work and a recent detailed study of the $^{14}\text{N}(^3\text{He},d)$ reaction [11] it is possible to extract the single particle centroid energies for the $2s_{1/2}$ and $1d_{5/2}$ single particle orbits in the $^{15}\text{N}-^{15}\text{O}$ pair. The single particle strengths for the two reactions are similar in terms of which states have the major single particle components but the absolute values for the ($^3\text{He},d$) reaction are on average only 65% of those extracted from the (d,p) analysis. Because ^{14}N has a ground state spin of 1, the determination of the energy weighted single particle energies (EWSPE) is slightly modified when compared to its determination from spin 0 targets and equation 3 of Ref. [23] is used to determine the values in the present work. The present $^{14}\text{N}(d,p)$ work showed there to be single neutron strength at higher excitation energies that would shift the centroid energies higher from those computed based on previous lower energy work. In addition the ($^3\text{He},d$) work limited its study to lower lying levels so that it is necessary to estimate where high lying single

IX. CONCLUSION

The present work reports new $^{14}\text{N}(\text{d},\text{p})$ data that find no narrow single neutron states occurring above about 12.5 MeV in excitation in contrast with multi-particle transfer reactions that populate a rich spectrum of states up to at least 20 MeV in excitation in ^{15}N . Shell model calculations that employ a cross shell $1\text{p}-2\text{s}1\text{d}$ interaction are able to reproduce and confirm the known ^{15}N positive and negative parity level scheme up to 11.5 MeV in excitation and are used to assign the spin-parity to a single particle level at 11.236 MeV in ^{15}N as well as to confirm the presence of a narrow level at 11.436 MeV of an alpha particle cluster nature. Knowledge of the spin-parities of the ^{15}N levels is then used to provide a complete set of spin-parities for its less well known mir-

ror, ^{15}O , up to 11 MeV in excitation. Figure 7 displays the calculated and final level schemes for these nuclei. The $2\text{s}_{1/2}$ and $1\text{d}_{5/2}$ single particle centroid neutron and proton energies show these orbits to be degenerate in the mass 15 system which means that these are the nuclei where the level ordering shifts between the lighter systems where the $2\text{s}_{1/2}$ orbit lies below that of the $1\text{d}_{5/2}$ orbit and the heavier system where the $1\text{d}_{5/2}$ orbit lies below that of the $2\text{s}_{1/2}$ orbit.

ACKNOWLEDGMENTS

This work was supported in part by the U.S. National Science Foundation.

-
- [1] E.C. Halbert and J.B. French, *Phys. Rev.* **105**, 1563 (1957).
 - [2] S.T. Hsieh and H. Horie, *Nucl. Phys.* **A151**, 243 (1970).
 - [3] S. Lie, T. Engeland and G. Dhall, *Nucl. Phys.* **A165**, 449 (1970).
 - [4] A.P. Shukla and G.E. Brown, *Nucl. Phys.* **A112**, 296 (1968).
 - [5] S. Lie and T. Engeland, *Nucl. Phys.* **A267**, 123 (1976).
 - [6] I. Tserruya, B. Rosner and K. Bethge, *Nucl. Phys.* **A213**, 22 (1973).
 - [7] H.G. Bingham, M.L. Halbert, D.C. Hensley, E. Newman, K.W. Kemper, and L.A. Charlton, *Phys. Rev.* **C11**, 1913 (1975).
 - [8] R.P. Beukens, T.E. Drake and A.E. Litherland, *Phys. Letts.* **56B**, 253 (1975).
 - [9] L.H. Harwood and K.W. Kemper, *Phys. Rev.* **C20**, 1383 (1979).
 - [10] F. Ajzenberg-Selove, *Nucl. Phys.* **A523**, 1 (1991).
 - [11] P.F. Bertone, A.E. Champagne, M. Boswell, C. Iliadis, S.E. Hale, V.Y. Hansper and D.C. Powell, *Phys. Rev.* **C66**, 055804 (2002).
 - [12] G.W. Phillips and W.W. Jacobs, *Phys. Rev.* **184**, 1052 (1969).
 - [13] C.R. Hoffman, B.P. Kay, and J.P. Schiffer, *Phys. Rev.* **C89**, 061305(R) (2014).
 - [14] C.E. Busch, T.B. Clegg, S.K. Datta and E.J. Ludwig, *Nucl. Phys.* **A223**, 183 (1974); N.J. Jarmie, J.H. Jett and R.J. Semper, *Phys. Rev.* **C10**, 1748 (1974).
 - [15] H. Ohnuma, N. Hosino, O. Mikoshiba, K. Raywood, A. Sakaguchi, G.G. Shute, B.M. Spicer, M.H. Tanaka, M. Tanifuji, T. Terasawa and M. Yasue, *Nucl. Phys.* **A448**, 205 (1985).
 - [16] Y. Utsuno and S. Chiba, *Phys. Rev.* **C83**, 021301(R) (2001).
 - [17] A. Volya, *Phys. Rev.* **C79**, 044308 (2009); <http://cosmo.volya.net>
 - [18] P.D. Kunz, <http://spot.colorado.edu/~kunz/DWBA.html>
 - [19] C.M. Vincent and H.T. Fortune, *Phys. Rev.* **C7**, 865 (1973).
 - [20] F. Perey and B. Buck, *Nucl. Phys.* **32**, 353 (1962).
 - [21] J.P. Schiffer, G.C. Morrison, R.H. Siemssen and B. Zeidman, *Phys. Rev.* **164**, 1274 (1967).
 - [22] A. Amokrane, M. Allab, H. Beaumevieuille, B. Faid, O. Bersillon, B. Chambon, D. Drain and J.L. Vidal, *Phys. Rev.* **C6**, 1934 (1972).
 - [23] S. Bedoor, A.H. Wuosmaa, J.C. Lighthall, M. Alcorta, B.B. Back, P.F. Bertone, B.A. Brown, C.M. Deibel, C.R. Hoffman, S.T. Marley, R.C. Pardo, K.E. Rehm, A.M. Rogers, J.P. Schiffer and D.V. Shetty, *Phys. Rev.* **C88**, 011304(R) (2013).
 - [24] T.R. Wang, R.B. Vogelaar and R.W. Kavanagh, *Phys. Rev.* **C43**, 883 (1991).
 - [25] G.A. Norton, K.W. Kemper, G.E. Moore, R.J. Puigh, and M.E. Williams-Norton, *Phys. Rev.* **C13**, 1211 (1976).